Interaction of Plasmon-Exciton at Interface of a Metal Thin Film and a C-Shaped Dielectric Columnar Thin Film Including Exciton Molecules

Ferydon Babaei*

Department of Physics, University of Qom, Qom, Iran

Corresponding author email: fbabaei@qom.ac.ir

Regular paper: Received: Apr. 29, 2022, Revised: Sep. 04, 2022, Accepted: Sep. 10, 2022,
Available Online: Sep. 12, 2022, DOI: 10.52547/ijop.16.1.37

ABSTRACT— In this study, the interaction of surface plasmon polariton and surface exciton at the interface of a plasmonic medium and a dielectric medium with a C-shaped column morphology consisting of exciton molecules theoretically and classically was investigated in the Kretschmann configuration using the transfer matrix method. The optical absorption spectra of surface plasmon polariton, surface exciton, and surface plexciton have been depicted. The results showed that when the surface plasmon polariton frequency is equal to or close to the frequency of the surface exciton, the polariton mode has two branches, high and low. The mode splitting is caused by the interaction of the surface plasmon polariton and the surface exciton. The characteristics of the splitting energy were analyzed at different structural parameters. The being surface of the plasmon, exciton, and plexciton waves and their localization at the interface between plasmonic and dielectric media were proved by the time averaged Poynting vector and the local absorption.

KEYWORDS: Kretschmann configuration, transfer matrix method, surface plexciton.

I. INTRODUCTION

Plasmon-exciton interaction is studied in new field of condensed matter physics called plexcitonics. A plexcitonic system includes a plasmonic medium (metal) and an excitonic medium (semiconductor). Whenever, plasmonic frequency of metal be close to excitonic frequency of semiconductor, a new quasiparticle called plexciton is created upon plasmon and exciton coupling [1-4]. Plexcitons are new hybrid optical modes divided into upper and lower polariton branches and the energy difference of polariton branches in plexciton absorption spectra is called Rabi Splitting energy regardless of plasmons and excitons damping in detuning frequency (the difference between frequency of plasmons and excitons) [5, 6].

Researchers have been looking for achieving high values of Rabi splitting energy in the field through proposed a special plexcitonic structure. High Rabi splitting energy will lead to strong coupling between plasmons and excitons [7]. In strong coupling regime, energy transfer between plasmons and excitons occurs in the order of femtoseconds [8]. Accordingly, this matter has been applied in nanolasers [9], biosensors [10], single photon switches [11], and spintronic [12].

In this work, the characteristics of plasmon-exciton interaction (surface plexciton excitation) were studied classically by transfer matrix method at interface of a metal thin film and a C-shaped columnar dielectric thin film including exciton molecules in Kretschmann configuration. The thin films with C-shaped columnar morphology are the kinds of new generation thin films called sculptured thin films [13]. The Optical absorption spectra as a function of incident light wavelength of linear P-polarization plane wave was depicted for different structural parameters in plasmonic, excitonic, and plexcitonic systems; and also, the

splitting of polariton peaks was analyzed. Preliminary theory for optical modeling is presented in Section 2 and followed by results and discussion in Section 3.

II. THEORY IN BRIEF

Consider a Kretschmann configuration as shown in Fig. 1. The region $0 \le z \le d_1$ is occupied by a metal with ε_{met} permittivity. Also, the region $d_1 \le z \le (d_1 + d_2)$ is occupied by a C-shaped columnar dielectric thin film including exciton molecules (TDBC) were self-assembly aggregated as J form in its pores.The $z \le 0$ and $z \ge (d_1 + d_2)$ regions are respectively, prism with refractive index of n_1 and air. The excitonic medium is a three-component composite includes air, exciton molecules and a C-shaped dielectric columns. Since the excitonic medium is a nonhomogeneous and anisotropic medium and we have to know its intrinsic properties including electrical permittivity ε and magnetic permeability μ for the light propagation. Exciton medium is considered as a non-permeable material ($\mu=\mu_0$).

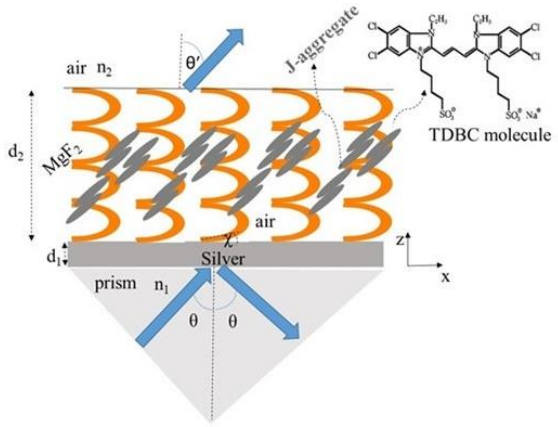

Fig. 1. A schematic of Kretschmann configuration for surface plexciton excitation at interface of a metal and a C-shaped columnar dielectric thin film including excitonic molecules as *J*, which is aggregated in pores of the dielectric medium.

To calculate the electric permittivity tensor of exciton medium, at first, the reference relative electric permittivity tensor of dielectric medium ε_{ref} including air and C-shaped dielectric columns is obtained by Bruggeman homogenization formalism in diagonal representation [13] and then:

$$\varepsilon_{ref} = \varepsilon_a u_z u_z + \varepsilon_b u_x u_x + \varepsilon_c u_y u_y, \quad (1)$$

where, $\varepsilon_{a,b,c}$ are the relative electric permittivity scalars and $u_{x,y,z}$ are Cartesian unit vectors. The relative electric permittivity scalars are as functions of wavelength and void volume fraction [13].

Assuming that the empty space of the medium is filled with a small fraction of f_j (percentage of excitonic pigments), then $f_j<<1$ and using Maxwell-Garnett Effective Medium theory [14], the relative electric permittivity scalars can be obtained as:

$$\varepsilon_{a,b,c}^{eff} = \varepsilon_{a,b,c}\left(1 + \frac{f_j}{(\varepsilon_{a,b,c}/(\varepsilon_j - \varepsilon_{a,b,c}) + (1-f_j)/3)}\right), \quad (2)$$

where, ε_j is the dielectric function of excitonic pigments. Now, using Oseen transformation [15], the effective electric permittivity tensor of excitonic medium can be obtained as below in rotating coordinate system:

$$\varepsilon_{ex} = S_y(\chi).\varepsilon_{ref}^{eff}.S_y^T(\chi), \quad (3)$$

where, $\chi = (\pi z/\Omega)$ is the rise angle of C-shaped dielectric columns relative to x- axis, Ω is the half structural period of C- shaped dielectric columns, and while the superscript T indicates to the transpose of a tensor. The $S_y(\chi)$ is rotation tensor of C –shaped dielectric columns to the y axis, and the ε_{ref}^{eff} is the effective electric permittivity tensor of excitonic medium in diagonal representation as follows:

$$S_y(\chi) = (u_x u_x + u_z u_z)\, cos\chi + (u_z u_x - u_x u_x)\, sin\chi + u_y u_y, \quad (4)$$

$$\varepsilon_{ref}^{eff} = \varepsilon_a{}^{eff} u_z u_z + \varepsilon_b{}^{eff} u_x u_x + \varepsilon_c{}^{eff} u_y u_y, \quad (5)$$

Suppose that the structure is exposed to a plane wave light with *P* linear polarization from prism side which is radiated with θ angle towards z- axis. Incident, reflected and transmitted electrical fields can be respectively described as follows:

$$\begin{cases} E_{inc}(r) = P_{inc}\, e^{i(k\,x + k_0\, n_1\, z\cos\theta)} & z \le 0 \\ E_{ref}(r) = \left(S\, r_S + P_{ref}\, r_P\right) e^{i(k\,x - k_0\, n_1\, z\cos\theta)} & z \le 0 \\ E_{tr}(r) = \left(S\, t_S + P_{tr}\, t_P\right) e^{i(k\,x + k_0\,(z - d_1 - d_2)\cos\theta')} & z \ge (d_1 + d_2) \end{cases}, \quad (6)$$

where, (r_s, r_p) and (t_s, t_p) are respectively the amplitudes of reflected and transmitted plane waves. Magnetic field in each medium can be obtained from $H(r) = (i\,\omega\mu_0)^{-1}\nabla \times E(r)$, and $k = k_0 n_1 \sin\theta$, and also k_0 is free wavenumber. The unit vectors for perpendicular and parallel of linear polarizations to incident light plane, *S*, $P_{inc,ref}$ and P_{tr} are as follows:

$$\begin{cases} S = u_y \\ P_{inc,ref} = \mp u_x \cos\theta + u_z \sin\theta, \\ P_{tr} = -u_x \cos\theta' + u_z \sin\theta' \end{cases} \quad (7)$$

where, $\sin\theta' = n_1 \sin\theta$ (Snell's Law), and $\cos\theta = +\sqrt{1 - \sin^2\theta'}$.

Reflection and transmission amplitudes can be obtained through continuity of tangential components of electromagnetic fields at interfaces from the following matrix equation:

$$\begin{bmatrix} t_S \\ t_P \\ 0 \\ 0 \end{bmatrix} = \left[K(\theta')\right]^{-1}.\left[T_{ex}\right].\left[T_{Met}\right].\left[K(\theta)\right].\begin{bmatrix} 0 \\ 1 \\ r_S \\ r_P \end{bmatrix}, \quad (8)$$

where *K*, T_{Met}, and T_{ex} are 4×4 matrices explained in details in the references [16, 17]. After calculation of reflection and transmission amplitudes with equation (8), optical absorption for *P* linear polarization can be obtained as $A = 1 - \sum_{i=s,p} R_i + T_i$, $i = s, p$, where the reflection and transmission is as $R_i = |r_i|^2$ and $T_i = \dfrac{\mathrm{Re}(\cos\theta')}{n_1 \cos\theta} |t_i|^2$, respectively.

III. RESULTS AND DISCUSSION

It should be mentioned here that for depiction the surface plasmon polariton (SPP) absorption spectra, we removed the exciton medium (C-shaped columnar thin film with J-aggregate TDBC dyes) from the proposed structure, and also to plot the surface exciton absorption spectra(X), we removed the plasmonic medium (Silver) from the structure (see Fig. 1). On the other hand, in depiction of the absorption spectra in all SPP and X plots, we did not consider the exciton medium and the plasmonic medium respectively in proposed structure. But in PLX plots, the absorption is given from the whole structure. All points related to the excitation of surface waves, such as the total internal reflection phenomenon and the fact that the angular position of the surface plasmon polariton and surface exciton peaks do not change to the dielectric medium thickness, have been taken into account in the calculations [16].

Excitation of surface plasmon polariton (SPP), surface exciton (X), and surface plexciton (PLX) waves is shown in Fig. 2 with fixed structural parameters $\theta = 25.6°$, $\Omega = 200nm$, N=3, $f_j = 0.052$, $f_v = 0.748$, $and\ n_1 = 2.57$ at different thicknesses of plasmonic medium (metal thin film), where Ω is the half structural period of C-shaped dielectric columns and *N* is their number. In our work, plasmonic medium was a silver thin film and also dielectric medium was a C-shaped magnesium fluoride columnar thin film. The angle of incidence light is chosen so that the plasmonic peak corresponds as close to or near the excitonic peak as possible. In Fig. 2(b), a peak is observed in plasmonic absorption spectra at 573nm wavelength, resulted from excitation of surface plasmon polariton at interface of metal and dielectric media. Excitonic spectra shows that a surface exciton wave has been excited at 591nm wavelength. From plexciton spectra it is observed that there are two polariton modes at 730nm (lower branch) and 583nm (upper branch) wavelengths. Separation of polariton mode into two branches is indicative of interaction between surface plasmon polariton and surface exciton.

The same behavior is seen in Fig. 2(c) as well. It must be noted that in calculating plasmonic and excitonic spectra, fraction of excitonic molecules and thickness of metal thin film have been respectively considered as equal to zero.

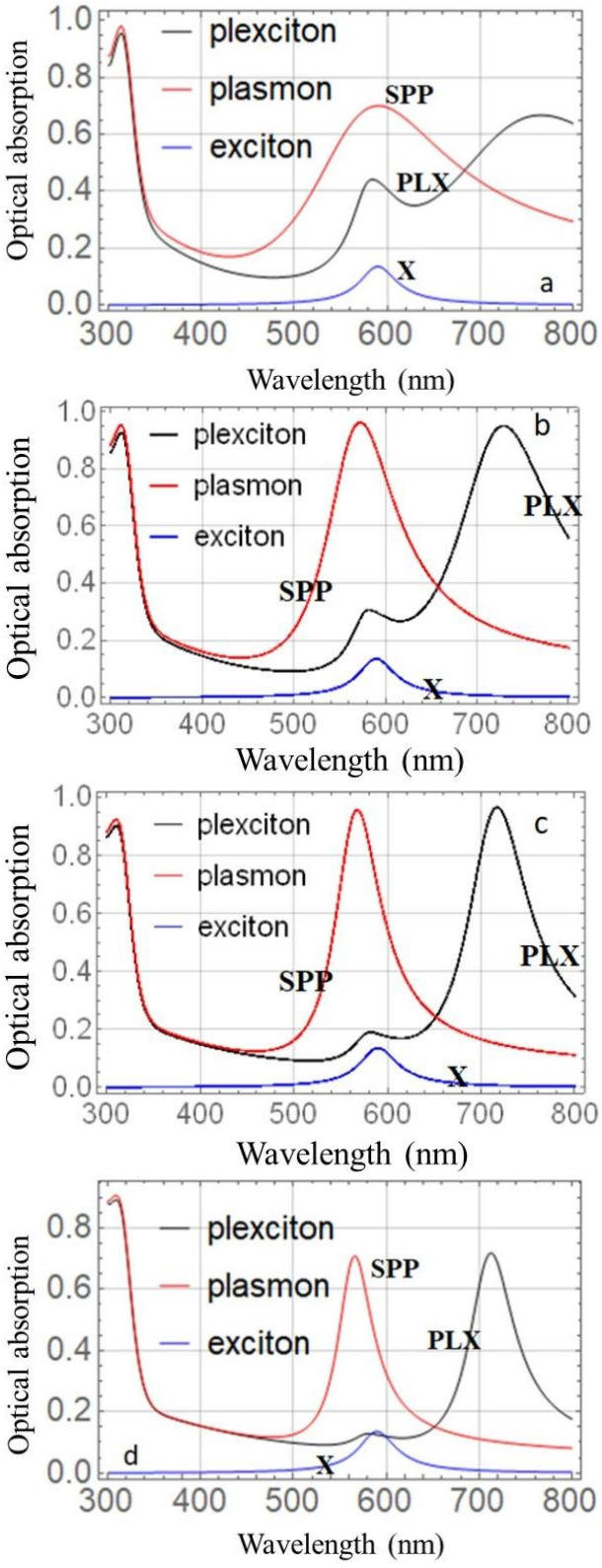

Fig. 2. Optical absorption spectra for excitation of surface plasmon polariton, surface exciton and surface plexciton with fixed parameters $\theta = 25.6°$, $\Omega = 200\,nm$, N=3, $f_j = 0.052$, $f_v = 0.748$, and $n_1 = 2.57$, for a) d1=30 nm, b) d1=40 nm, c) d1=50 nm, and d) d1=60 nm.

To understand better, the effect of plasmonic thickness on surface waves, it has been changed from 30 to 60nm and obtained the results are provided in the Fig. 2. It was observed that with increase of metal thickness from 30 to 40nm, separation between polariton branches increased and then it decreased within the range of 50 to 60nm. The obtained results showed that the maximum absorption intensity in plasmonic spectra occurred at 40nm metal thickness in our work which is equal to saturation thickness of metal thin film for excitation of surface plasmon polariton. Upon thickness increase of metal thin film from 50 to 60nm, absorption intensity of the peak decreased and position of plasmonic peak shifted towards larger wavelengths. So, under the above conditions, d_1=40 nm is saturation thickness of metal thin film, because, upon change of thickness from this value, the optical absorption decreased. This is because if the thickness of the metal is less than the thickness of the saturation, a large fraction of the incident light transmits and the surface plasmon cannot be coupled to the exciton at this time. Contrarily, if the thickness of the metal is greater than the thickness of the saturation, due to the increase in the tunneling distance, the excitation of surface plasmon polaritons at the interface is decreased and the energy of photons is damped in the metal. Therefore, when thickness of metal layer is close to that of saturation thickness, maximum splitting is observed between polariton peaks in plexcitonic spectra.

In Fig. 3, the effect of fraction of excitonic molecules on optical absorption spectra is shown for excitation of plasmon polariton, exciton, and plexciton: a) f_j=0.062, f_v=0.738 and b) f_j=0.042, f_v=0.758. The Other parameters are same as Fig. 2 except the thickness of metal thin film was 40nm and the total fraction of excitonic molecules and porosity was fixed and equal to 0.8. The peak of plasmonic spectra is located at 573nm wavelength in Fig. 3(a). Also, there are two completely distinguished peaks in plexciton plot that the polariton peaks are located at 774 and 583nm wavelengths. However, the peak of excitonic spectra is occurred at 591nm wavelength. The same pattern is observed in Fig. 3(b) as well. Here,

fraction of excitonic molecules decreased from 0.062 to 0.032, however, in Fig. 3 it has been always *fj*+*fv*=0.8 and only two of them are presented in the Fig. 3. The results show that upon increase of fraction of excitonic molecules, the splitting between polariton branches is increased. As it is observed, excitonic medium had three components: columnar dielectric thin film, air, and exciton molecules. The reason for increase of splitting in polariton branches is increase of the strength of dipole moment excitons at interface which is created due to aggregation of air molecules on excitons.

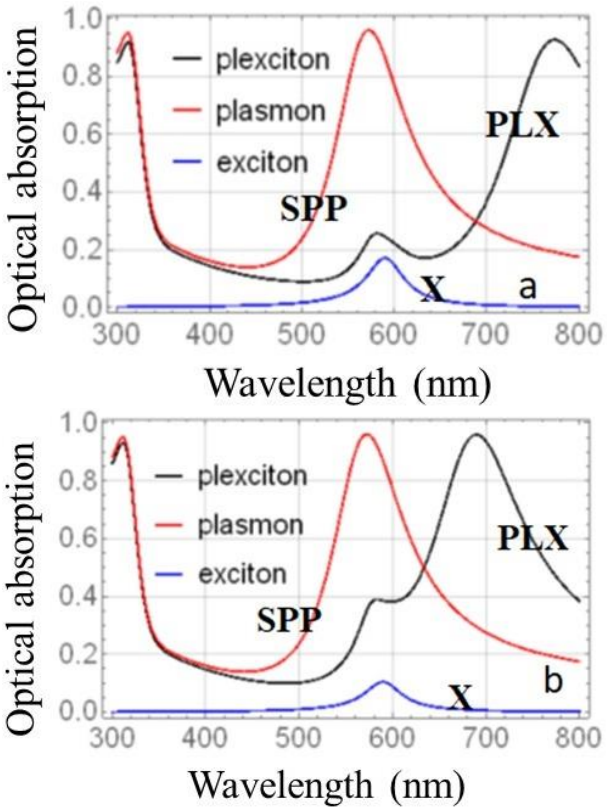

Fig. 3. Optical absorption spectra for excitation of surface plasmon polariton, surface exciton and surface plexciton, a) $f_j = 0.062$, $f_v = 0.738$, and b) $f_j = 0.042$, $f_v = 0.758$. The else parameters are same as Fig. 2 except d1=40 nm.

One of the characteristics of C- shaped columnar dielectric thin film is its porosity that can be effective on light propagation. As we know, in order of the surface wave propagation at the interface between the two media, the angle of incident light must be greater than the critical angle so that the total internal reflection phenomenon can occur. Porosity of columnar dielectric thin film is effective on refractive index of dielectric medium and critical angle here can be obtained from $\theta_{spp} \cong \sin^{-1}\sqrt{\frac{\max(\varepsilon_a,\varepsilon_b,\varepsilon_c)}{\varepsilon_1}}$. In Fig. 4, the effect of porosity on excitation of surface waves is shown for two different values. At f_v=0.2, maximum plasmonic absorption occurs at 558nm and maximum excitonic absorption occurs at 590nm, whereas, plexciton absorption spectrum had two separate peaks at 717 and 580nm wavelengths. At f_v=0.4, the plasmonic and excitonic spectra had a peak at 590 nm, and in plexcitonic absorption spectra, we saw two distinct peaks at 717 and 580 nm. Here also, different porosity values from 20 to 80% were studied and it became clear that upon increase of porosity of dielectric medium, the plasmon damping and refractive index of dielectric thin film decreased. This matter leads to decrease of critical angle. In zero porosity, the host medium will have maximum density i.e. the same homogenous and isotropic state. Where, porosity will be increased from zero on, the thin film is diluted and refractive index is decreased as a result. Therefore, change of porosity is effective on location of plasmonic peaks and it is also effective on splitting of polariton modes in plexcitonic spectra.

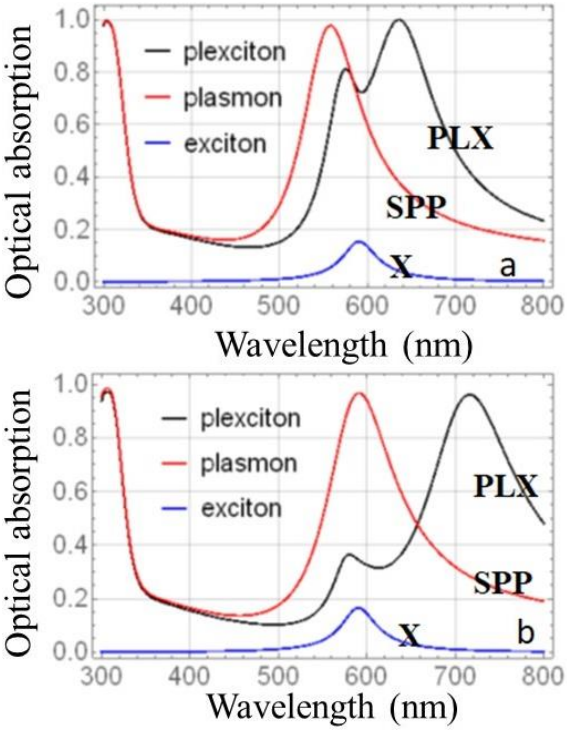

Fig. 4. Optical absorption spectra for excitation of surface plasmon polariton, surface exciton and

surface plexciton, a) $\theta = 33°$, $f_j = 0.1$, and $f_v = 0.1$, and b) $\theta = 30°$, $f_j = 0.08$, and $f_v = 0.32$. The other parameters are the same as those in Fig. 3.

In Fig. 5, the effect of refractive index of prism on splitting of polariton modes was studied. Parameters are similar to the Fig. 2(a). In n_1=1.52 plasmonic absorption spectra had a peak at 593nm and also the excitonic absorption spectra had a peak at 591 nm. Plexciton absorption plot had two polariton branches with higher peak and absorption intensity of 96% at 766nm and shorter peak with absorption intensity of 22% at 584nm. At this case, frequency detuning angle was 47°. In Fig. 5(b) (n_1=2), plasmonic spectra shows a peak at 563nm with absorption intensity of 97% and the exciton spectra also shows a peak at 591nm with absorption intensity of 11%. High peak of plexcitonic spectra is located at 704nm with absorption intensity of 98% and shorter peak is located at 583nm with absorption intensity of 35%. Here, it is observed that frequency detuning angle was decreased with increase of refractive index of the prism, reaching to 34°. On the other hands, it can be expressed that upon decrease of the prism refractive index, the distance between polariton branches remains constant but the zero detuning angle frequency ($\omega_{SPP} = \omega_X$) shifts to higher angles. In previous figures with refractive index of the prism (n_1=2.57), the zero detuning angle was $\theta = 25.6°$. Then, peaks of surface plasmon polariton shift to higher angles for coupling to excitons. Also, it is observed that upon increase of the prism refractive index, absorption intensity will not be changed at plasmonic peaks, however, the position of the peaks inclined to lower wavelengths. Then, the refractive index of prism is a very important parameter. Because, due to limitation in measurement of plasmonic modes at higher incident angles in Kretschmann configuration, excitation angles can be lowered through selection of a prism with high refractive index. Therefore, displacement of plasmonic peaks is effective on splitting of polariton modes at plexcitonic spectra.

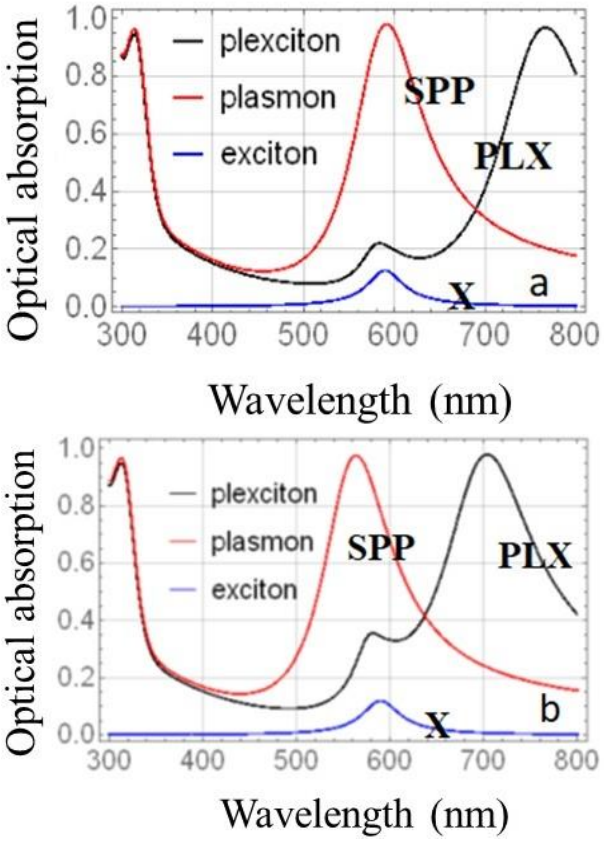

Fig. 5. Optical absorption spectra for excitation of surface plasmon polariton, surface exciton and surface plexciton, a) $\theta = 47°$ and $n_1 = 1.52$, and b) $\theta = 34°$ and $n_1 = 2$. The other parameters are similar to those in Fig. 2.

In order to the effect of structural period (pitch) and numbers of periods of dielectric columns on excitation of surface plasmon polariton, exciton, and plexciton, the optical absorption spectra are shown in Fig. 6 for a) N=4, b) N=4.5, c) Ω=150nm, and d) Ω=250nm. The else structural parameters are the same as those in Fig. 2.

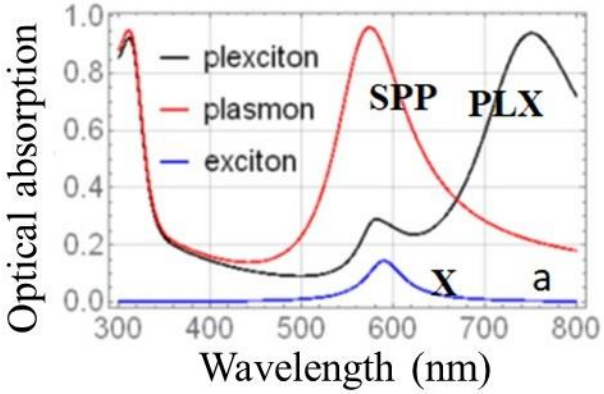

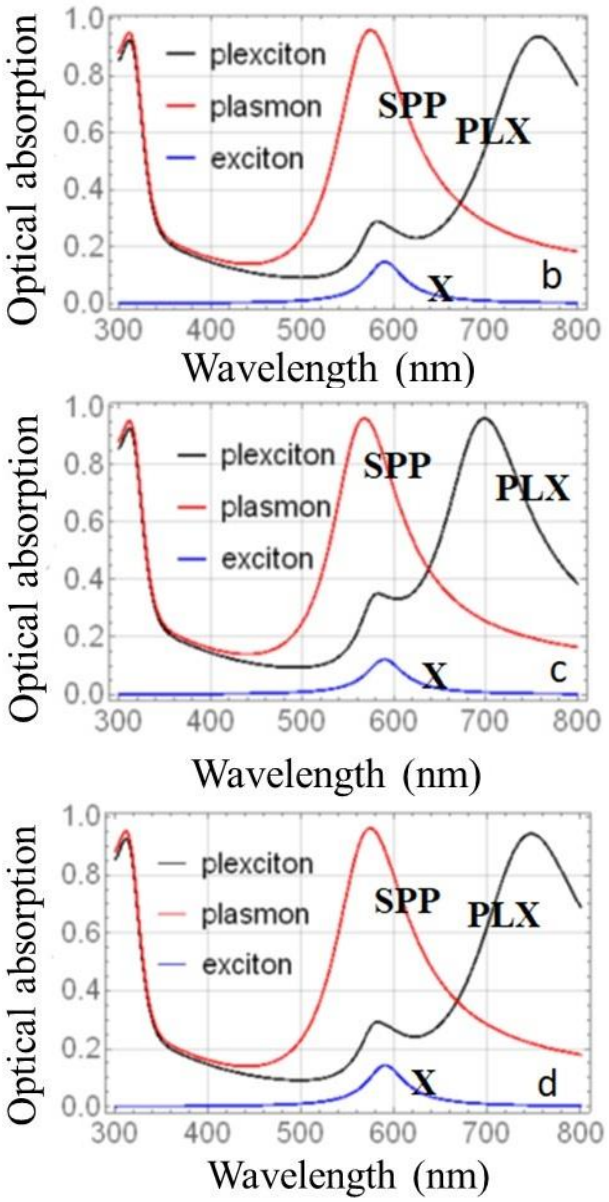

Fig. 6. Optical absorption spectra for excitation of surface plasmon polariton, surface exciton and surface plexciton, a) N=4, b) N=4.5, c) Ω=150nm, and d) Ω=250nm. The Other parameters are similar to those in Fig. 2.

In Fig. 6(a) with Np=4, the plasmonic peak in SPP spectra is located at 576nm and the excitonic peak is occurred in X spectra at 589nm. PLX absorption plot shows two peaks that the higher is located at 753nm and the shorter is occurred at 583nm. In Fig. 6(b) where Np=4.5, the same trend is observed. Then, it became clear that the increase of structural period has not much effect on position and intensity of plasmonic peaks, however, a saturation thickness can be considered for C-shaped columnar thin film after which plasmonic absorption intensity remains fixed upon increase of structural period. Therefore, it can be concluded that this quantity has not much effect on splitting between polariton modes in plexcitonic spectra. In Fig. 6(c) where Ω=150nm, the plot of plasmonic absorption had a peak at 568nm and also the excitonic spectra had a peak at 591nm, whereas, in plexcitonic spectra two separate peaks are observed. The higher peak with absorption intensity of 96% occurs at 700nm and shorter peak with absorption intensity of 34% happens at 581nm.

At half structural period Ω=250nm (Fig. 6(d)), a maximum absorption has been observed at plasmonic spectra with absorption intensity of 96% at 575nm, and also in excitonic plot a maximum absorption was observed at 588nm with absorption intensity of 14%. At plexcitonic spectra also two separate peaks were obtained so that the splitting between polariton branches has been increased. According to the results, by increasing of structural period, the position of plasmonic peak shifts to higher wavelengths. After 250nm by increase of structural period, no tangible change is observed in position and absorption intensity of the peaks. Therefore, it can be concluded that in this work, Ω=250nm is a saturated structural period.

To more analysis of the localization of surface waves at interface of plasmonic and excitonic media, the time averaged Poynting vector components ($\mathbf{P}$), and local absorption ($-\nabla.\mathbf{P}$) as a function of depth structures are depicted in Fig. 7, when a surface plasmon polariton wave in Figs. 7(a) and 7(b), a surface exciton wave in Figs. 7(c) and 7(d) and a surface plexciton wave in Figs. 7(e) and 7(f) are excited and the other parameters similar as Fig. 2. According to the results, the surface plasmon polariton and surface exciton waves are localized at interface of metal and columnar thin film and they are damped by moving away from interface. Comparison between SPP, X and PLX plots shows that the absorption intensity at plexcitonic spectra was increased at interface relative to exciton spectra. Therefore, it can be concluded that the energy of surface plasmon polariton was decreased and transferred to excitons and there is a hybridization between

plasmon polariton and exciton due to coupling between surface plasmon polariton and surface exciton.

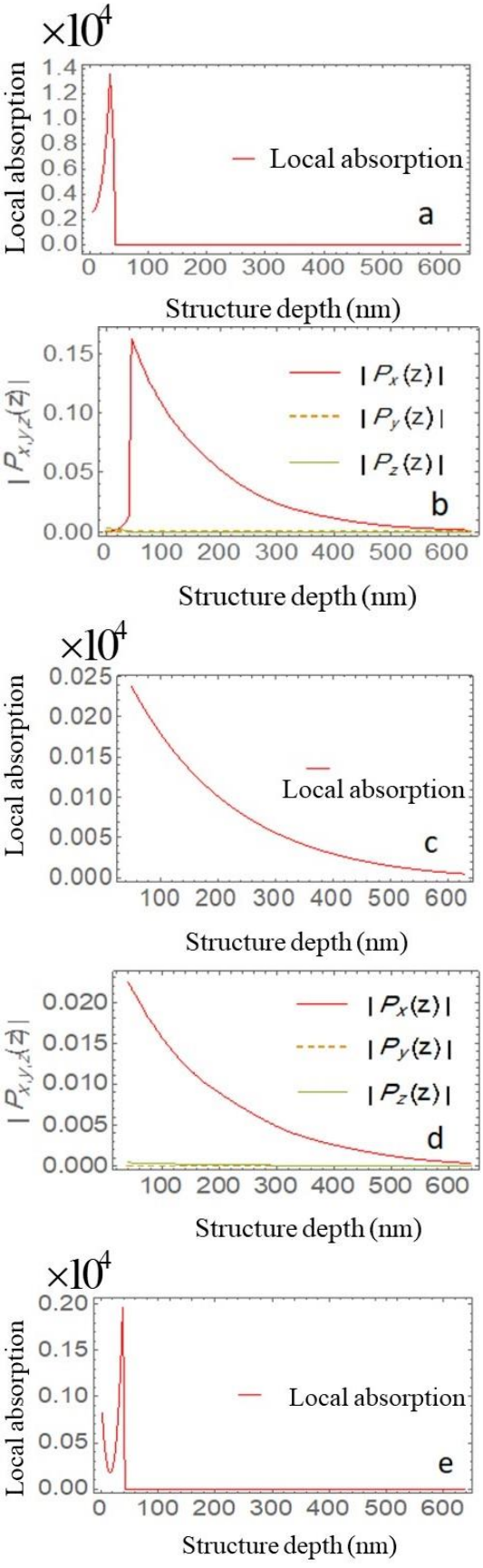

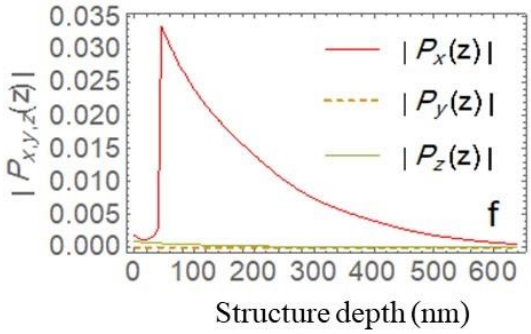

Fig. 7. The time averaged of Poynting vector components and local absorption as a function of structure depth when a surface plasmon polariton wave (a, b), a surface exciton wave (c, d), and a surface plexciton wave (e, f) are excited. The other parameters are same as Fig. 2.

IV. CONCLUSION

The excitation of surface plasmon polariton, surface exciton, and surface plexciton waves at planar interface of a silver thin film and a C-shaped magnesium fluoride dielectric thin film including excitonic molecules in the Kretschmann configuration using transfer matrix method were investigated. The obtained results showed that the selection of a metal thin film with 40 nm thickness causes a maximum splitting energy between polariton branches in plexcitonic spectra. It became clear that the polariton branches get away from each other by the increasing of fraction of excitonic molecules in dielectric medium. It was found that as the porosity of dielectric medium increases, the plasmonic peaks tend towards higher wavelengths and also the critical angles for total internal reflection phenomenon become smaller, followed by affected splitting between polariton branches. Also, our calculations revealed that the incident light angle for match frequencies between plasmon polariton and exciton was shifted to larger angles by decreasing the refractive index of prism. We found that the surface plasmon polariton, surface exciton, and surface plexciton waves are localized at interface of plasmonic and excitonic media by the depiction of the time-averaged Poynting vector components as a function of structure depth. Finally, the comparison between local absorption of surface plasmon polariton, surface exciton, and surface plexciton spectra showed that the energy of surface plasmon

polariton at interface is decreased and it has been transferred to surface excitons; which is resulted from them being coupled at the interface and a new optical quasiparticle of surface plexciton being created.

ACKNOWLEDGMENT

This work was carried out with the support of the University of Qom.

REFERENCES

[1] M. Pelton and M. Sheldon, "Plasmon-exciton coupling" Nanophotonics, Vol. 8, pp. 513-516, 2019.

[2] Y. Niu, H. Xu, and H. Wei, "Unified Scattering and Photoluminescence Spectra for Strong Plasmon-Exciton Coupling," Phys. Rev. Lett., Vol. 128, pp. 167402 (1-5), 2022.

[3] M. Kumar, J. Dey, S. Swaminathan, and M. Chandra, "Shape Dependency of the Plasmon–Exciton Interaction at the Nanoscale: Interplay between the Plasmon Local Density of States and the Plasmon Decay Rate," J. Phys. Chem. C, Vol. 126, pp. 7941–7948, 2022.

[4] D. Melnikau, P. Samokhvalov, A. Sánchez-Iglesias, M. Grzelczak, I. Nabiev, and Y.P. Rakovich, "Strong coupling effects in a plexciton system of gold nanostars and J-aggregates," J. Luminescence, Vol. 242, pp. 118557 (1-7), 2022.

[5] S. Balci, C. Kocabas, S. Ates, E. Karademir, O. Salihoglu, and A. Aydinli, "Tuning surface plasmon-exciton coupling via thickness dependent plasmon damping," Phys. Rev. B, Vol. 86, pp. 235402 (1-6), 2012.

[6] S. Balci, "Ultrastrong plasmon–exciton coupling in metal nanoprisms with J-aggregates," Opt. Lett., Vol. 38, pp. 4498-4501, 2013.

[7] G. Zengin, M. Wersäll, S. Nilsson, T.J. Antosiewicz, M. Käll, and T. Shegai, "Realizing strong light-matter interactions between single-nanoparticle plasmons and molecular excitons at ambient conditions," Phys. Rev. Lett., Vol. 114, pp. 157401 (1-14), 2015.

[8] P. Vasa, W. Wang, R. Pomraenke, M. Lammers, M. Maiuri, C. Manzoni, G. Cerullo, and C. Lienau, "Real-time observation of ultrafast Rabi oscillations between excitons and plasmons in metal nanostructures with J-aggregates," Nature Photon., Vol. 7, pp. 128-132, 2013.

[9] V.S. Lebedev and A.S. Medvedev, "Plasmon—exciton coupling effects in light absorption and scattering by metal/J-aggregate bilayer nanoparticles," Quantum Electron., Vol. 42, pp. 701 (1-13), 2012.

[10] T. Srivastava and R. Jha, "Tailoring surface plasmon-exciton polariton for high-performance refractive index monitoring," J. Opt., Vol. 23, pp. 045001 (1-8), 2021.

[11] J. Sun, Y. Li, H. Hu, W. Chen, D. Zheng, S. Zhang, and H. Xu, "Strong plasmon–exciton coupling in transition metal dichalcogenides and plasmonic nanostructures," Nanoscale, Vol. 13, pp. 4408-4419, 2021.

[12] P. Yin, Y. Tan, H. Fang, M. Hegde, and P.V. Radovanovic, "Plasmon-induced carrier polarization in semiconductor nanocrystals," Nature nanotechnol., Vol. 13, pp. 463-467, 2018.

[13] A. Lakhtakia and R. Messier, " Sculptured thin films: Nanoengineered morphology and optics," Vol. 143. SPIE Press, 2005.

[14] J.C. Hernández and J.A. Reyes, "Optical band gap in a cholesteric elastomer doped by metallic nanospheres," Phys. Rev. E, Vol. 96, pp. 062701 (1-11), 2017.

[15] I. Jánossy, *Optical effects in liquid crystals*, Vol. 5, Springer Science and Business Media, 2013.

[16] J. Polo, T. Mackay, and A. Lakhtakia, "Electromagnetic surface waves: a modern perspective," Newnes, 2013.

[17] F. Babaei and M. Rostami, "Excitation of surface plexciton wave at interface of a metal and a columnar thin film infiltrated with J-aggregate dyes," Opt. Commun., Vol. 439, pp. 8-15, 2019.

Ferydon Babaei was born in Talesh in 1974. He received PhD degree in optics of sculptured thin films from University of Tehran in 2008. Then he joined the University of Qom. Now he studies the plasmonic properties and interaction of plasmon – exciton characteristics in nanostructures and thin films. He has published more than 40 papers in international journals